

AD-A235 184

2



PENNSTATE



Applied Research Laboratory

BACKSCATTERING FROM ROUGH INTERFACES AND THE PARABOLIC APPROXIMATION

S. T. McDaniel

Technical Memorandum
File No.91-104
12 April 1991

Copy No. 19

DTIC
ELECTE
MAY 02 1991
S D

APPLIED RESEARCH LABORATORY
STATE COLLEGE, PA 16804
(814) 865-3031

Applied Research Laboratory
P.O. Box 30
State College, PA 16804
(814) 865-3031

91 4 22 046

PENNSTATE



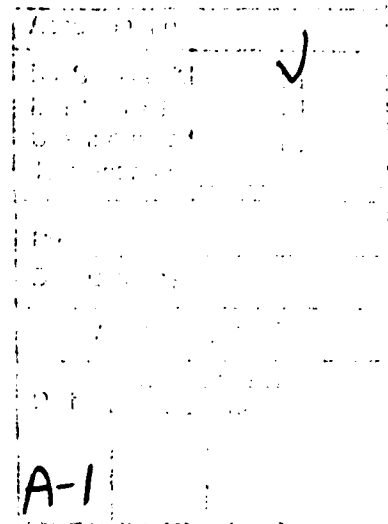
Applied Research Laboratory

BACKSCATTERING FROM ROUGH INTERFACES AND THE PARABOLIC APPROXIMATION

S. T. McDaniel

Technical Memorandum
File No. 91-104
12 April 1991

Copy No. / 9



Dist. A. Per telecon Mr. M. Orr
ONR/Code 11250A

CG 51/91

Applied Research Laboratory
P.O. Box 30
State College, PA 16804
(814) 865-3031

Backscattering from Rough Interfaces and the Parabolic Approximation

S. T. McDaniel

Abstract:

Iterative solutions of coupled parabolic wave equations are examined to determine the validity of applying this method to predict low frequency ocean acoustic reverberation. Solutions for backscattering from a random rough interface between two media of differing wave number are obtained in the form of an expansion in powers of the rough interface excursion from its mean value. This expansion is found to differ significantly from the corresponding expansion obtained by applying perturbation theory to the full elliptic wave equation.

TABLE OF CONTENTS

	<u>Page</u>
Abstract.....	1
Introduction.....	2
I. General Formulation.....	3
II. Backscatter from Rough Interfaces.....	4
A. The Transmitted Field.....	4
B. The Backscattered Field.....	6
C. Backscattering Strength.....	8
III. Comparisons with Perturbation Theory.....	11
A. Bragg Scattering.....	11
B. Higher Order Scattering.....	13
IV. Discussion.....	15
Acknowledgement.....	15
Appendix A.....	16
Appendix B.....	18
References.....	20

LIST OF FIGURES

Figure 1 Procedure for Iterative Solution of the Parabolic Equation.....	21
Figure 2 Backscattering Geometry.....	22
Figure 3 Bragg Scattering Predicted by PE and PT for a Ten Degree Critical Angle.....	23
Figure 4 Comparison of PE and PT Bragg Backscatter for a Critical Angle of Five Degrees.....	24
Figure 5 PE vs PT Bragg Backscatter for an Angle of Intromission of Five Degrees.....	25
Figure 6 Higher Order (2,2) Contributions to Backscatter for a Critical Angle of Ten Degrees.....	26
Figure 7 Fourth Order Backscattering Strength Predictions for a Critical Angle of Ten Degrees.....	27

INTRODUCTION

The parabolic approximation has been successfully applied to electromagnetic propagation¹, non-linear acoustic phenomena², and underwater acoustic transmission³. Claerbout⁴ appears to first have considered iterative solution of a coupled pair of parabolic equations to obtain the backscattered field applicable to seismic reflection profiling. Because the parabolic approximation provides a computationally efficient numerical method for solving wave propagation and scattering problems, its applicability to underwater acoustic backscatter is well worth investigating.

In this article, a two-dimensional pair of coupled parabolic equations is considered. The solution to this pair of equations is obtained for backscattering from a random rough interface between two media of the same density but differing indices of refraction. To facilitate comparison with other scattering theories, results are obtained for a plane wave incident on a rough surface area in the far field of a receiver, and ensemble averaged.

Perturbation theory, which agrees well with exact Monte-Carlo simulations of scattering from pressure release⁵ and fluid-solid⁶ interfaces of moderate roughness, is used for comparison. For the lowest order scattering which is due to Bragg diffraction, the parabolic and perturbation results are found to differ significantly. Higher order scattering terms are also evaluated with similar findings.

Section I of this article presents the general formulation of the problem in which the elliptic wave equation is split to obtain a coupled pair of parabolic equations. In Section II, this coupled pair of equations is solved to obtain the backscattered field. Numerical comparisons between perturbation theory and the results of Section II are presented in Section III. Section IV summarizes and discusses the results.

I. GENERAL FORMULATION

The two-dimensional wave equation in a medium having a variable index of refraction $k(x,z)$ is considered

$$\left[\frac{\partial^2}{\partial x^2} + \frac{\partial^2}{\partial z^2} + k^2(x,z) \right] v = 0, \quad (1)$$

where v is the acoustic pressure. For acoustic energy propagating close to the x direction, it is convenient to rewrite this equation in matrix form as

$$\frac{\partial}{\partial x} \begin{pmatrix} v \\ \frac{\partial v}{\partial x} \end{pmatrix} = \begin{pmatrix} 0 & 1 \\ -A^2 & 0 \end{pmatrix} \begin{pmatrix} v \\ \frac{\partial v}{\partial x} \end{pmatrix}, \quad (2)$$

where $A^2 = k^2(x,z) + \partial^2/\partial z^2$. Equation (2) may be split by a method due to Coronas⁷ to obtain a pair of coupled equations for the transmitted and reflected fields, v_+ and v_- respectively, where

$$\begin{pmatrix} v_+ \\ v_- \end{pmatrix} = T \begin{pmatrix} v \\ \frac{\partial v}{\partial x} \end{pmatrix}, \quad (3)$$

and T is the splitting matrix. Claerbout's⁴ result follows from the choice

$$T = \begin{pmatrix} 1 & -i/A \\ 1 & +i/A \end{pmatrix}. \quad (4)$$

Substitution of Eq. (3) into Eq. (2), then yields the following pair of equations

$$\frac{\partial v_+}{\partial x} = -\frac{1}{2} A^{-1} \frac{\partial A}{\partial x} (v_+ - v_-) + i A v_+, \quad (5)$$

$$\frac{\partial v_-}{\partial x} = +\frac{1}{2} A^{-1} \frac{\partial A}{\partial x} (v_+ - v_-) - i A v_-. \quad (6)$$

Equations (5) and (6) are exact; no approximations have been made up to this point. However, to obtain an efficient numerical solution of this pair of equations, it is usually assumed that the reflected field is small and may be neglected in the solution of Eq. (5), or that

$$\frac{\partial v_r}{\partial x} = -\frac{1}{2} A^{-1} \frac{\partial A}{\partial x} v_r + iA v_r, \quad (7)$$

which with a suitable approximation for A , may be solved for the transmitted field. With the transmitted field known, the reflected field may be found by solving Eq. (6).

This procedure for numerically solving Eqs. (6) and (7) is illustrated schematically in Figure 1. A parabolic equation is numerically solved for the transmitted field v_t out to some maximum range of interest. Values of v_t are stored at each point where $\partial A/\partial x$ is nonvanishing. Equation (6) is then solved for the reflected field with the initial condition that $v_r = 0$ at the maximum range of interest. If desired, with v_r known, one may return to Eq. (5) to refine the estimates of v_t , and iterate again to better estimate v_r . This method is certainly numerically tractable for scattering from rough interfaces, since only the transmitted and reflected fields on the interfaces need be stored.

II. BACKSCATTER FROM ROUGH INTERFACES

A. The Transmitted Field

To determine if the method described in Section I does indeed provide a good estimate of the reverberant field, we consider scattering at an interface between two media having the same density but differing indices of refraction. For simplicity, an incident plane wave is assumed as illustrated in Figure 2.

To obtain an expression for the transmitted field, the operator A is approximated as

$$A = k(x, z) + \frac{1}{2k_0} \frac{\partial^2}{\partial z^2} , \quad (8)$$

where k_0 is a reference wave number. In Appendix A, it is shown that the first term on the right-hand side of Eq. (7) contributes negligibly to backscattering. With the neglect of this term, the transmitted field above the interface $v_*^{(1)}$ then obeys

$$\left(\frac{\partial}{\partial x} - iK_1 - \frac{i}{2k_0} \frac{\partial^2}{\partial z^2} \right) v_*^{(1)} = 0 , \quad (9)$$

and below the interface $v_*^{(2)}$ obeys

$$\left(\frac{\partial}{\partial x} - iK_2 - \frac{i}{2k_0} \frac{\partial^2}{\partial z^2} \right) v_*^{(2)} = 0 , \quad (10)$$

where K_1 and K_2 are respectively, the (constant) indices of refraction above and below the interface.

For an incident plane wave

$$v_{in} = \exp [i(kx - k_1 z)] , \quad (11)$$

$v_*^{(1)}$ and $v_*^{(2)}$ are given by

$$\begin{aligned} v_*^{(1)} = & \exp(ikx) [\exp(-ik_1 z) + R \exp(ik_1 z)] \\ & + \int_0^{\infty} dk' \exp[i(k'x + k'_1 z)] u_1(k') , \end{aligned} \quad (12)$$

and

$$v_1^{(2)} = T \exp[i(kx - k_2 z)] + \int_0^{\infty} dk' \exp[i(k'x - k_2' z)] u_2(k') , \quad (13)$$

where $k_j = [2k_0(K_j - k)]^{1/2}$, and

$$R = (k_1 - k_2) / (k_1 + k_2) ,$$

$$T = 2k_1 / (k_1 + k_2) .$$

The quantities $u_1(k')$ and $u_2(k')$ may be expanded in a functional series in the rough surface extension $\zeta(x)$ from its mean value. Following Kuperman⁸, one obtains

$$u_1(k') = (k_2' - k_1') T \left\{ i h(k' - k) + \int_{-\infty}^{\infty} dk'' h(k' - k'') h(k'' - k) \left[k_1'' - k_2'' + \frac{(k_2 + k_2')}{2} \right] + \dots \right\} , \quad (14)$$

$$u_2(k') = (k_2' - k_1') T \left\{ i h(k' - k) + \int_{-\infty}^{\infty} dk'' h(k' - k'') h(k'' - k) \left[k_1'' - k_2'' + \frac{(k_2 - k_1')}{2} \right] + \dots \right\} , \quad (15)$$

where $h(k)$ is defined by

$$\zeta(x) = \int_{-\infty}^{\infty} dk h(k) \exp(ikx) . \quad (16)$$

B. The Backscattered Field

To obtain the backscattered field, A is approximated as in Eq. (8) and the term $v \cdot \partial A / \partial x$ appearing on the right-hand side of Eq. (6) is neglected (see Appendix B), whence $v^{(1)}$ obeys

$$\left(\frac{\partial}{\partial x} + iK_1 + \frac{i}{2k_0} \frac{\partial^2}{\partial z^2} \right) v_-^{(1)} = A^{-1} \frac{\partial A}{\partial x} v_+^{(1)} / 2, \quad (17)$$

in medium 1. The solution to this equation is

$$v_-^{(1)}(x, z) = \iint_{-\infty}^{\infty} dx' dz' A^{-1} \frac{\partial A}{\partial x} v_+^{(1)}(x', z') G_-^{(1)}[(x-x'), (z-z')]/2, \quad (18)$$

where the Green's function $G_-^{(1)}$ is given by

$$G_-^{(1)} = - [k_0/2\pi(x'-x)]^{1/2} \exp\{-i[\pi/4 + K_1(x-x') + k_0(z-z')^2/2(x-x')]\}, \quad (19)$$

for $(x-x') \leq 0$ and vanishes otherwise. The geometry of Figure 2 will be considered, with the receiver at $x=0, z=z_0$, and the scattering region located at $x' = L \pm \Delta x/2$, where $L \gg \Delta x$ and $\Delta x \gg \lambda$, the acoustic wave length.

In this case $G_-^{(1)}$ may be simplified

$$G_-^{(1)} \approx - (k_0/2\pi L)^{1/2} \exp\{i[\phi + K_1 x' - k_0 z_0 z'/L]\}, \quad (20)$$

where $\phi = -\pi/4 + k_0 z_0^2/2L$ and $k_0 z'^2/2L$ is neglected, since, as is apparent below, the only values of z' that contribute are on the rough interface $z' = \zeta(x')$.

For an interface between two media,

$$k(x, z) = K_1 H[z - \zeta(x)] + K_2 H[\zeta(x) - z], \quad (21)$$

where $H(x) = \begin{cases} 1, & x \geq 0 \\ 0, & x < 0 \end{cases}$.

With the definition of A, and Eq. (21)

$$\frac{A^{-1}}{2} \frac{\partial A}{\partial x} = \frac{1}{2} A^{-2} k(x, z) (K_2 - K_1) \delta[z - \zeta(x)] \frac{\partial \zeta}{\partial x}. \quad (22)$$

The scattered field may then be found by substituting Eqs. (12), (20) and (22) into Eq. (19)

$$v_{-}^{(1)}(0, z_0) = (K_2 - K_1) \int_{L-\Delta x/2}^{L+\Delta x/2} dx' \frac{k[x', \zeta(x')]}{2} \frac{\partial \zeta(x')}{\partial x'} G_{-}^{(1)} A^{-2} v_{+}[x', \zeta(x')] , \quad (23)$$

where the integration over the rough surface has been replaced with an integration along the x' axis.

By expanding the exponentials that appear in v_{+} and G_{-} as a power series in the surface excursion, the corresponding series for v_{-} may be obtained. In the following, we can approximate $k[x', \zeta(x')] A^{-2}$ as $1/K_1$ since only low grazing angles are of interest. With these approximations

$$v_{-}^{(1)}(0, z_0) = Q \int_{L-\Delta x/2}^{L+\Delta x/2} dx' \frac{\partial \zeta(x')}{\partial x'} \exp(iK_1 x') (\alpha_1 + \alpha_2 + \alpha_3 + \dots) , \quad (24)$$

where

$$\begin{aligned} \alpha_1 &= (1+R) \exp(ikx') , \\ \alpha_2 &= -i\zeta(x') \exp(ikx') [k_1(1-R) + (k_0 z_0/L)(1+R)] \\ &\quad + iT \int_0^{\bar{}} dk' \exp(ik'x') (k_2' - k_1') h(k' - k) , \\ \alpha_3 &= -\zeta^2(x') \exp(ikx') [(k_0 k_1 z_0/L)(1-R) + (k_1^2 + k_0^2 z_0^2/L^2)(1+R)/2] \\ &\quad + T \int_0^{\bar{}} dk' \exp(ik'x') (k_2' - k_1') \left\{ \int_{\bar{}} dk'' h(k' - k'') h(k'' - k) \left[k_1'' - k_2'' + \frac{(k_2 + k_2')}{2} \right] \right. \\ &\quad \left. - \zeta(x') (k_1' - k_1) h(k' - k) \right\} , \end{aligned} \quad (25)$$

$$\text{and } Q = \frac{-(K_2 - K_1)}{2K_1} \left(\frac{k_0}{2\pi L} \right)^{1/2} e^{i\phi} .$$

C. Backscattering Strength

It is evident from Eq. (24) that $v_{-}^{(1)}$ has the form

$$v_-^{(1)} = w_1 + w_2 + w_3 + \dots \quad (26)$$

where the subscript on w denotes its order in the rough surface excursion from its mean value. The expectation $\langle \rangle$ of the scattered intensity is then given by

$$\langle v_-^{(1)} v_-^{*(1)} \rangle = \langle w_1 w_1^* \rangle + \langle w_2 w_2^* \rangle + \langle w_1 w_3^* \rangle + \langle w_1^* w_3 \rangle + \dots \quad (27)$$

The first term on the right-hand side of this expression is the Bragg scattering term and is the major contributor to backscatter for slightly rough surfaces. The remaining terms are higher order corrections which become important for moderately rough surfaces. For very rough surfaces, one expects the series to diverge as it does in perturbation theory.

Substituting Eq. (16) into Eqs. (24) and (25), yields

$$\langle w_1 w_1^* \rangle = (\Delta x/L) [(K_2 - K_1)(K_1 + k)]^2 k_0 T T^* W(K_1 + k) / [4(2)^{1/2} K_1^2] \quad (28)$$

where $\zeta(x)$ has been assumed Gaussian with

$$\langle h(k) h^*(k') \rangle = W(k) \delta(k - k') \quad ,$$

and the rms surface excursion σ obeys

$$\sigma^2 = \int_{-\infty}^{+\infty} dk W(k) \quad .$$

The factor of $(2)^{1/2}$ appearing in the denominator of Eq. (28) arises from considering a Gaussian illumination pattern as in Reference 9.

Before continuing, note that some simplifications result if monostatic backscatter is considered and k_0 is selected equal to k so that $k_0 z_0/L = k_1$.

In this case

$$\begin{aligned} \langle w_2 w_2^* \rangle &= 8\pi \Delta x k_1^2 Q Q^* \int_{-x}^{\infty} dk' W(k') W(2k+k') \\ &\times \{4k^2 - 2k^2 [f(k') + f^*(k')] + [k^2 + (k+k')^2] f(k') f^*(k')\} / (2)^{1/2}, \end{aligned} \quad (29)$$

where $f(k') = (k_2' - k_1') / (k_2 + k_1)$, and

$$\begin{aligned} \langle w_3 w_1^* \rangle &= 8\pi \Delta x k^2 Q Q^* T^* W(2k) \{-2k_1^2 \sigma^2 \\ &+ T \int_{-\infty}^{\infty} dk' W(k+k') [k_2(k_2 - k_1) + (K_1' - K_2') (K_1' + k_2 - 2k_1)]\} / (2)^{1/2}, \end{aligned} \quad (30)$$

where $K_j' = [2k_0(K_j - k' - 2k)]^{1/2}$.

To obtain Eqs. (29) and (30), we have used

$$\begin{aligned} \langle h(k) h(k') h(k'') h(k''') \rangle &= W(k) W(k'') \delta(k+k') \delta(k''+k''') \\ &+ W(k) W(k') [\delta(k+k'') \delta(k'+k''') + \delta(k+k''') \delta(k'+k'')] , \end{aligned}$$

and $h(k) = h^*(-k)$. It has also been assumed that $\Delta x \gg L_c$ the rough surface correlation length, and that $K_1 \approx k$.

Finally, the scattering strength S_{PE} may be obtained from $\langle v_-^{(1)} v_-^{(1)*} \rangle$

$$S_{PE} = (L/\Delta x) \langle v_-^{(1)} v_-^{(1)*} \rangle . \quad (31)$$

It is worthwhile remarking that the dominant contributions to Eqs. (29) and (30) arise from the first terms in curly brackets on the right-hand sides of these expressions. The remaining terms are negligible for the cases considered in the following section. Physically these terms and the contributions discussed in Appendix A correspond to multiple forward scatter and shadowing.

III. COMPARISONS WITH PERTURBATION THEORY

A. Bragg Scattering

Analogous to the development of Section II A for the parabolic equation (PE), in perturbation theory (PT), the pressure p in the upper and lower media due to an incident plane wave

$$p_{in} = \exp[i(kx - \kappa_1 z)] , \quad (32)$$

may be expressed as

$$p_1 = \exp(ikx) [\exp(-i\kappa_1 z) + R_0 \exp(i\kappa_1 z) + \int_{-\infty}^{\infty} dk' \exp[i(k'x + \kappa_1' z)] q_1(k') , \quad (33)$$

and

$$p_2 = T_0 \exp[i(kx - \kappa_2 z)] + \int_{-\infty}^{\infty} dk' \exp[i(k'x - \kappa_2' z)] q_2(k') , \quad (34)$$

where $\kappa_1 = (K_1^2 - k^2)^{1/2}$, and R_0 and T_0 are the Rayleigh reflection and transmission coefficients.

Again, following Kuperman, a functional series for the q_j may be derived. The backscattering strength is then found from

$$S_{PT} = \kappa_1 \sin\theta \langle q_1(-k) q_1^*(-k) \rangle . \quad (35)$$

The lowest order contribution to q_1 is

$$q_1(-k) = -2i\kappa_1 R_0 h(-2k) , \quad (36)$$

and the corresponding backscattering strength is

$$S_{PT}(1,1) = 4\kappa_1^3 R_0^2 \sin\theta W(2k) . \quad (37)$$

The analogous Bragg term for the PE case can be written

$$S_{PE}(1,1) = 4k_1^2 \frac{(K_2 - K_1)^2}{|k_2 + k_1|^2} \frac{k_0(K_1 + k)^2}{4(2)^{1/2} K_1^2} W(k + K_1) . \quad (38)$$

On comparing Eqs. (37) and (38), it is evident that the functional dependence of the two expressions differs at low grazing angles with Eq. (37) varying with the fourth power of the grazing angle and Eq. (38) with the second power.

To illustrate the differences in the PE and PT Bragg results, we consider a surface wave number spectrum $W(k)$ obeying

$$W(k) = c/k^3 , \quad K_L < |k| < K_m , \quad (39)$$

which yields a result that is independent of frequency at lowest order.

Figure 3 compares the PE and PT predictions for $c = 0.001$ and $K_2/K_1 = 0.985$ corresponding to a critical angle of ten degrees. Although the two curves are similar, differences of approximately 10 dB occur at the critical angle and at very low grazing angles. Figures 4 and 5 compare the results for a critical angle of five degrees, and an angle of intromission of five degrees, $K_2/K_1 = 0.996$ and 1.004 , respectively. Even for these cases, where the scattering is weak, significant differences between the two predictions are apparent.

In Figures 3, 4, and 5, $k_0 = K_1$. From the definition of k_1 and k_2 , and Eq. (38), it is clear that k_0 is a multiplicative factor, and that adjusting this factor within reasonable limits will not significantly alter the results. Thus, the disparity between the PE and PT Bragg scattering predictions does not appear to be a consequence of the angular propagation error inherent in the parabolic approximation.

It is evident from the analysis of Section II that each operation by the operator $\partial A/\partial x$ introduces a factor of ζ in the solution of Eqs. (5) and (6) for backscattering from rough interfaces. Hence, although a number of

approximations have been made in obtaining Eq. (38), none of these approximations affects this lowest order, or Bragg scattering result. It is also clear that repeated iteration of Eqs. (5) and (6), as described in Section I, can only lead to terms of higher order in the surface excursion. It thus appears that solution of the full coupled pair of equation is needed to accurately model Bragg diffraction.

B. Higher Order Scattering

For moderately rough surfaces, higher order terms in PT lead to enhanced scattering. The second order contribution to q_1 is

$$q_1(-k) = 2\kappa_1 R_0 \int_{-\infty}^{\infty} dk' h(-k-k') h(k'-k) (\kappa_2 + \kappa'_1 - \kappa'_2) , \quad (40)$$

and the corresponding backscattering strength is

$$S_{PT}(2,2) = 16\kappa_1^3 R_0^2 \sin^2 \theta \int_0^{\infty} dk' W(k+k') W(k-k') |\kappa'_1 - \kappa'_2 + \kappa_2|^2 . \quad (41)$$

The comparable PE prediction is

$$S_{PE}(2,2) = (L/\Delta x) \langle w_2 w_2^* \rangle , \quad (42)$$

where $\langle w_2 w_2^* \rangle$ is given by Eq. (29).

To compare the predictions of Eqs. (41) and (42), we select $K_L = 0.01 K_1$ and $K_M = 2K_1$ in Eq. (39). This choice provides predictions independent of frequency and corresponds to an rms roughness $\sigma = 14$ m for a frequency of 200 Hz. Figure 6 compares the (2,2) PE and PT results for a ten degree critical angle. As in Figure 3, the PE predictions exceed the PT result at very low grazing angles and are significantly lower near the critical angle.

It is also of interest to examine the remaining terms that contribute to the fourth order scattering strength prediction. The third order contribution of q_1 takes the form

$$\begin{aligned}
 q_1(-k) = & 2i\kappa_1 R_0 \int dk' dk'' h(-k-k') h(k'-k'') h(k''-k) \\
 & \times \left[(\kappa_2' - \kappa_1') \left(\frac{\kappa_2}{2} + \kappa_1'' - \kappa_2'' \right) + \frac{\kappa_1' \kappa_2' (\kappa_2' - \kappa_1')}{2(\kappa_2' + \kappa_1')} - k' \frac{(k+k')}{2} + k \frac{(k''-k)}{2} \right. \\
 & \left. - \frac{(\kappa_2^2 + \kappa_1 \kappa_2 + \kappa_1^2)}{6} + \frac{(\kappa_2'^2 - \kappa_1'' \kappa_2'' + \kappa_1'^2)}{2} - k''(k'-k'') - \frac{\kappa_2^2}{3} - \frac{\kappa_2(\kappa_1'' - \kappa_2'')}{2} \right].
 \end{aligned} \tag{43}$$

The scattering strength is then given by

$$\begin{aligned}
 S_{PT}(1,3) = & 4\kappa_1^2 R_0 R_0^* W(-2k) \int_{-\infty}^{\infty} dk' W(k-k') \left[\frac{-\kappa_1^2 \kappa_2}{(\kappa_2 + \kappa_1)} + \frac{\kappa_1' \kappa_2' (\kappa_2' - \kappa_1')}{(\kappa_2' + \kappa_1')} \right. \\
 & \left. - (\kappa_2' - \kappa_1') (\kappa_2' - \kappa_1') + (\kappa_1'^2 - \kappa_1' \kappa_2' + \kappa_2'^2) + 2\kappa_1 (\kappa_2' - \kappa_1') \right],
 \end{aligned} \tag{44}$$

where $\kappa_j' = [K_j^2 - (k' - 2k)^2]^{1/2}$. The corresponding result for the PE case is

$$S_{PE}(1,3) = (L/\Delta x) \langle w_1 w_3^* \rangle, \tag{45}$$

where $\langle w_1 w_3^* \rangle$ is given by Eq. (30).

Figure 7 compares the full fourth order scattering strength predictions for a critical angle of ten degrees for $c = 0.001$ and the same choice of K_L and K_M as in Figure 6. For PT, the sum of Eqs. (37), (41), and (44) plus its complex conjugate is shown. The PE result is the sum of Eqs. (38), (42), and (45) plus its complex conjugate. In the PT case, the (1,3) plus (3,1) contributions are positive below the critical angle, and negative above it. The corresponding PE contributions are negative at all grazing angles, hence the increased disparity slightly below the critical angle.

IV. DISCUSSION

A coupled pair of parabolic equations has been solved for the intensity backscattered from a random rough interface. The result has been expressed in the form of a series in the rough interface excursion for comparison with the results of perturbation theory. Even the lowest order, or Bragg, term in the parabolic approximation differs significantly from the perturbation theory result. Because all terms of the first order have been retained in the iterative solution of the parabolic equations, this disparity can only be attributed to the original splitting of the elliptic wave equation and neglect of the backscattered field in the initial solution for the transmitted field. Higher order corrections to the scattering strength follow the same trends as the Bragg terms, with significant differences between the parabolic and perturbation results.

The parabolic approximation offers several advantages for studying scattering from rough interfaces: it is computationally efficient, includes a full diffractive treatment of shadowing effects, and can handle focusing effects at the scattering surface. For these reasons it is useful in the study of forward scatter for which its predictions are in good agreement with perturbation theory. However, due to the disparities noted above, iterative solutions are of doubtful utility for the study of reverberation.

ACKNOWLEDGEMENT

This research was performed at the Applied Research Laboratory of The Pennsylvania State University under the support of the Office of Naval Research.

APPENDIX A

To estimate the results of including the term $-A^{-1}\partial A/\partial x v_+/2$ on the right-hand side of Eq. (7) consider

$$v_+ = \bar{v}_+ + \bar{v}'_+ ,$$

where to lowest order, from Eq. (12)

$$\bar{v}_+ = T \exp(ikx) ,$$

and \bar{v}'_+ is treated as a small perturbation, obeying

$$\left(\frac{\partial}{\partial x} - iA\right)\bar{v}'_+ = - (K_2 - K_1) \delta[z - \zeta(x)] \frac{\partial \zeta(x)}{\partial x} \frac{\bar{v}_+}{2K_1} . \quad (\text{A-1})$$

The appropriate Green's function for the solution of Eq. (A-1) is

$$G_+ = [k(x, z)/2\pi(x-x')]^{1/2} \exp\{i[\pi/4 + k(x, z)(x-x') + k_0(z-z')^2/2(x-x')]\} , \quad (\text{A-2})$$

for $0 < x' < x$. To proceed, we select $k_0 = K_1$ and approximate $k(x, z) = K_1$.

Solving Eq. (A-1) via Eq. (A-2), then yields

$$\bar{v}'_+(x, \zeta) = Q'T \int_0^x dx' \frac{\partial \zeta'}{\partial x'} (x-x')^{-1/2} \exp\{iK_1[x' + (\zeta - \zeta')^2/2(x-x')]\} , \quad (\text{A-3})$$

where $Q' = (L)^{1/2}Q$. Neglecting the second factor in the exponential of Eq. (A-3) is valid for small surface slopes. Then by using Eq. (16) for $\zeta(x)$ and making the change of variables $x' = x - q$, Eq. (A-3) takes the form

$$\bar{v}'_+(x, \zeta) = Q'T \int_{-\infty}^{\infty} ik'dk' h(k') \exp[ix(K_1 + k')] \int_0^x \frac{dq}{Q'^{1/2}} \exp(-iqk') . \quad (\text{A-4})$$

Extending the upper limit of the q integral to ∞ , then yields

$$\tilde{v}_-(x, \zeta) = Q'T \int_{-\infty}^{\infty} ik'dk'h(k') \exp[ix(K_1 + k') + iS\pi/4] (\pi/2|k'|)^{1/2}, \quad (\text{A-5})$$

where $S = 1$ for $k' < 0$ and $S = -1$ for $k' > 0$.

To lowest order, the resultant backscattered field $\tilde{v}_-(0, z_0)$ is given, from Section II B, by

$$\tilde{v}_-(0, z_0) = Q \int_{L-\Delta x/2}^{L+\Delta x/2} dx' \frac{\partial \zeta(x')}{\partial x'} \exp(iK_1 x') \tilde{v}_-[x', \zeta(x')]. \quad (\text{A-6})$$

Substituting Eq. (A-5) into Eq. (A-6), yields

$$\tilde{v}_- = QQ'T \int_{L-\Delta x/2}^{L+\Delta x/2} dx' \frac{\partial \zeta(x')}{\partial x'} \exp(2iK_1 x') \int_{-\infty}^{\infty} ik'dk'h(k') \exp(ixk' + iS\pi/4) (\pi/2|k'|)^{1/2}. \quad (\text{A-7})$$

On comparing Eq. (A-7) with the α_2 term of Eq. (24), it is apparent that an additional factor of Q' appears in \tilde{v}_- . Because $|K_1 - K_2|/K_1 \ll 1$, in the examples treated, the contributions arising from the \tilde{v}_- term are negligible.

One may verify this computationally by evaluating such terms as

$$\begin{aligned} \langle \tilde{v}_- \tilde{v}_-^* \rangle &= |QQ'T|^2 \pi^2 \Delta x \int_0^{\infty} dk' W(K_1 - k') W(K_1 + k') \\ &\times [(K_1 - k')^2 |K_1 + k'| + (K_1 + k')^2 |K_1 - k'| + 2(K_1^2 - k'^2)^{1/2} H(K_1 - k')] / (2)^{1/2}. \end{aligned}$$

APPENDIX B

Following the method of Appendix A, the result of retaining the term $-A^{-1}\partial A/\partial x v_-/2$ on the right-hand side of Eq. (6) may be estimated by considering

$$v_- = \bar{v}_- + \vartheta_- , \quad (\text{B-1})$$

where

$$\bar{v}_- = \int dx' dz' A^{-1} \frac{\partial A}{\partial x} v_-^{(1)}(x', z') G_-(x-x', z-z')/2 , \quad (\text{B-2})$$

and

$$\vartheta_- = -\int dx' dz' A^{-1} \frac{\partial A}{\partial x} \bar{v}_-(x', z') G_-(x-x', z-z')/2 . \quad (\text{B-3})$$

For $x' > x$, to lowest order

$$\bar{v}_-(x, \zeta) = Q'T \int_0^x \frac{dx'}{(x'-x)^{1/2}} \frac{\partial \zeta(x')}{\partial x'} \exp iK_1(2x'-x) , \quad (\text{B-4})$$

where $k_0 = K_1$ and $k(x, z) = K_1$. Equation (B-4) may be integrated, as in Appendix A, yielding

$$\bar{v}_-(x, \zeta) = i(\pi/2)^{1/2} Q'T \int_{-\infty}^{\infty} \frac{k' dk' h(k')}{|k' + 2K_1|^{1/2}} \exp[i(k'x + K_1x + S\pi/4)] , \quad (\text{B-5})$$

where $S = -1$ for $(k' + 2K_1) < 0$, and $S = +1$ for $(k' + 2K_1) > 0$. Substituting Eq. (B-5) into Eq. (B-3), then yields

$$\begin{aligned} \vartheta_-(0, z_0) = & -i(\pi/2)^{1/2} QQ'T \int_{L-\Delta x/2}^{L+\Delta x/2} dx' \frac{\partial \zeta(x')}{\partial x'} \int_{-\infty}^{\infty} \frac{k' dk' h(k')}{|k' - 2K_1|^{1/2}} \\ & \times \exp[ix'(2K_1 + k') + iS\pi/4] . \end{aligned} \quad (\text{B-6})$$

As an example, we consider the expectation $\langle \bar{v}_- v_- \rangle$ to which only the α_2 term of Eq. (24) contributes

$$\begin{aligned} \langle \bar{v}_- v_- \rangle &= QQ^* Q' T 4 \Delta x \pi^{3/2} k_1 K_1 \int_{-\infty}^{\infty} dk' W(k') W(2K_1 + k') \\ &\times Sk' |2K_1 + k'|^{1/2} \exp(iS\pi/4) , \end{aligned} \tag{B-7}$$

which is smaller by a factor of approximately $(1 - K_1/K_2)$ than the contribution of Eq. (29).

REFERENCES

1. V. A. Fock, Electromagnetic Diffraction and Propagation Problems (Pergamon, New York, 1965).
2. V. P. Kuznetsov, "Equations of Non-linear Acoustics," *Sov. Phys. Ac.* 16, 467-470 (1971).
3. D. Lee and S. T. McDaniel, Ocean Acoustic Propagation by Finite Difference Methods (Pergamon, New York, 1988).
4. J. F. Claerbout, "Coarse Grid Calculations of Waves in Inhomogeneous Media with Application to Delineation of Seismic Structure," *Geophys.* 35, 407-418 (1970).
5. E. I. Thorsos, "Acoustic Scattering from a 'Pierson-Moskowitz' Sea Surface," *J. Acoust. Soc. Am.* 88, 335-349 (1990).
6. D. H. Berman, "Simulations of Rough Interface Scattering," *J. Acoust. Soc. Am.* 89, 623-636 (1991).
7. J. Coronas, "Bremmer Series that Correct Parabolic Approximations," *J. Math. Anal. Appl.* 50, 161-168 (1975).
8. W. A. Kuperman, "Coherent Component of Specular Reflection and Transmission at a Randomly Rough Two-Fluid Interface," *J. Acoust. Soc. Am.* 58, 365-370 (1975).
9. S. T. McDaniel, "Diffractive Corrections to the High-Frequency Kirchhoff Approximation," *J. Acoust. Soc. Am.* 79, 952-957 (1986) [see the Appendix].

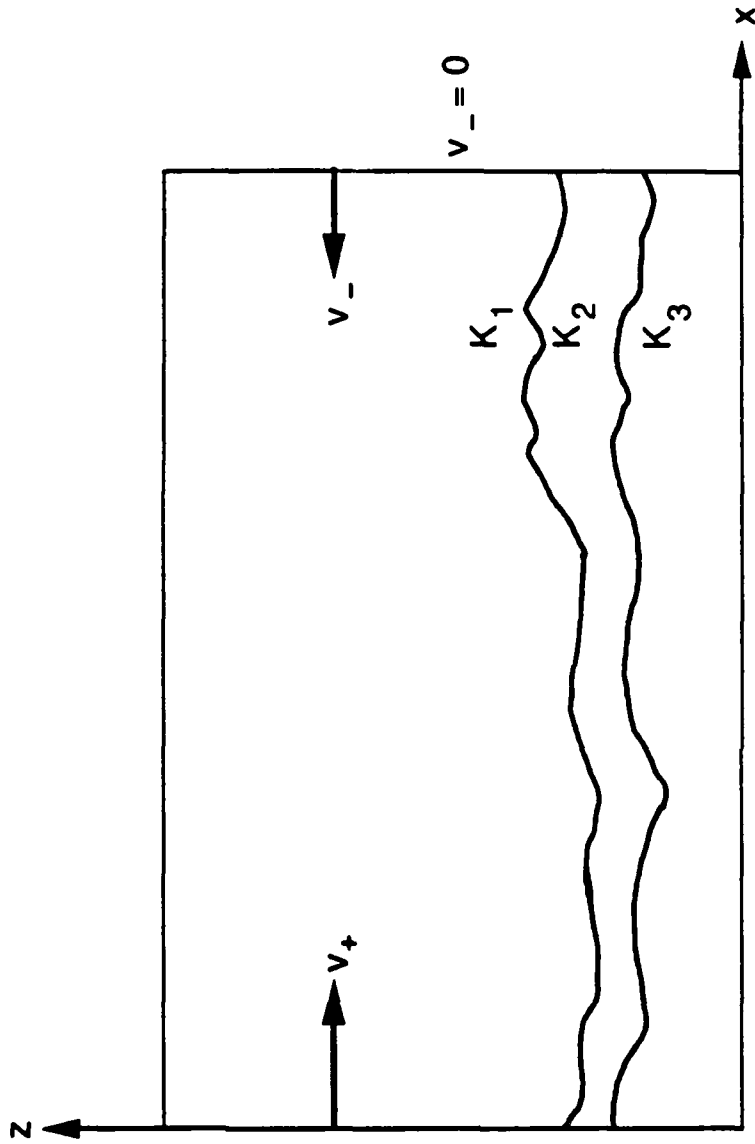


Figure 1. Procedure for Iterative Solution of the Parabolic Equation.

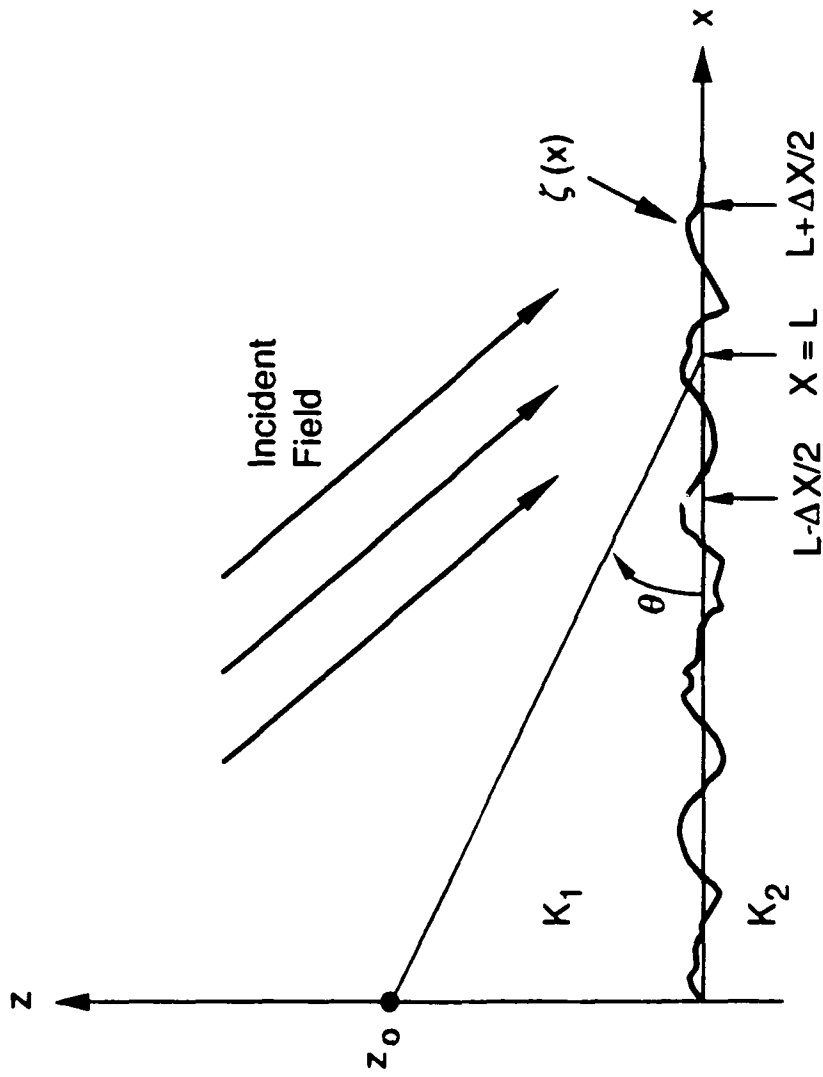


Figure 2. Backscattering Geometry.

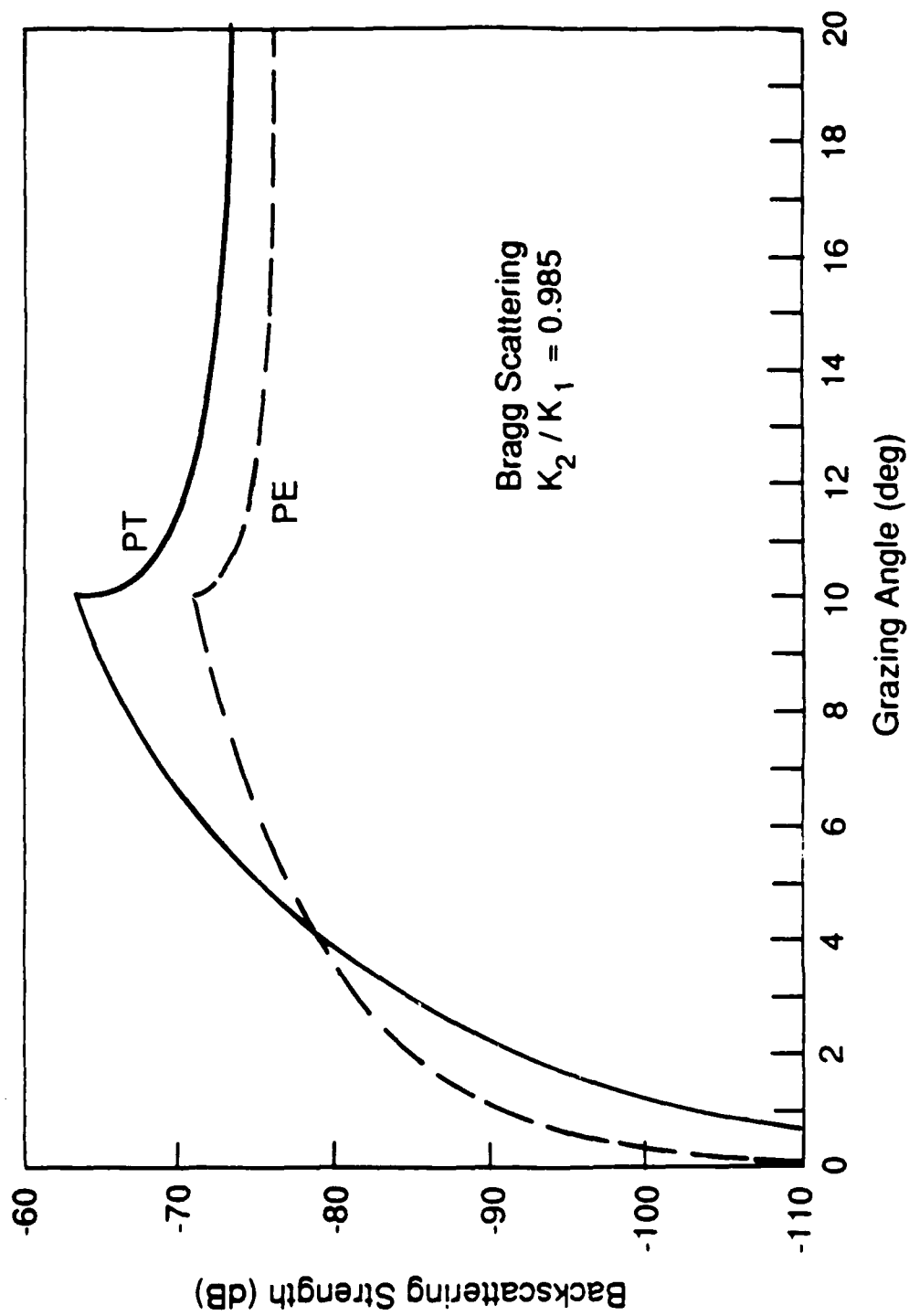


Figure 3. Bragg Scattering Predicted by PE and PT for a Ten Degree Critical Angle.

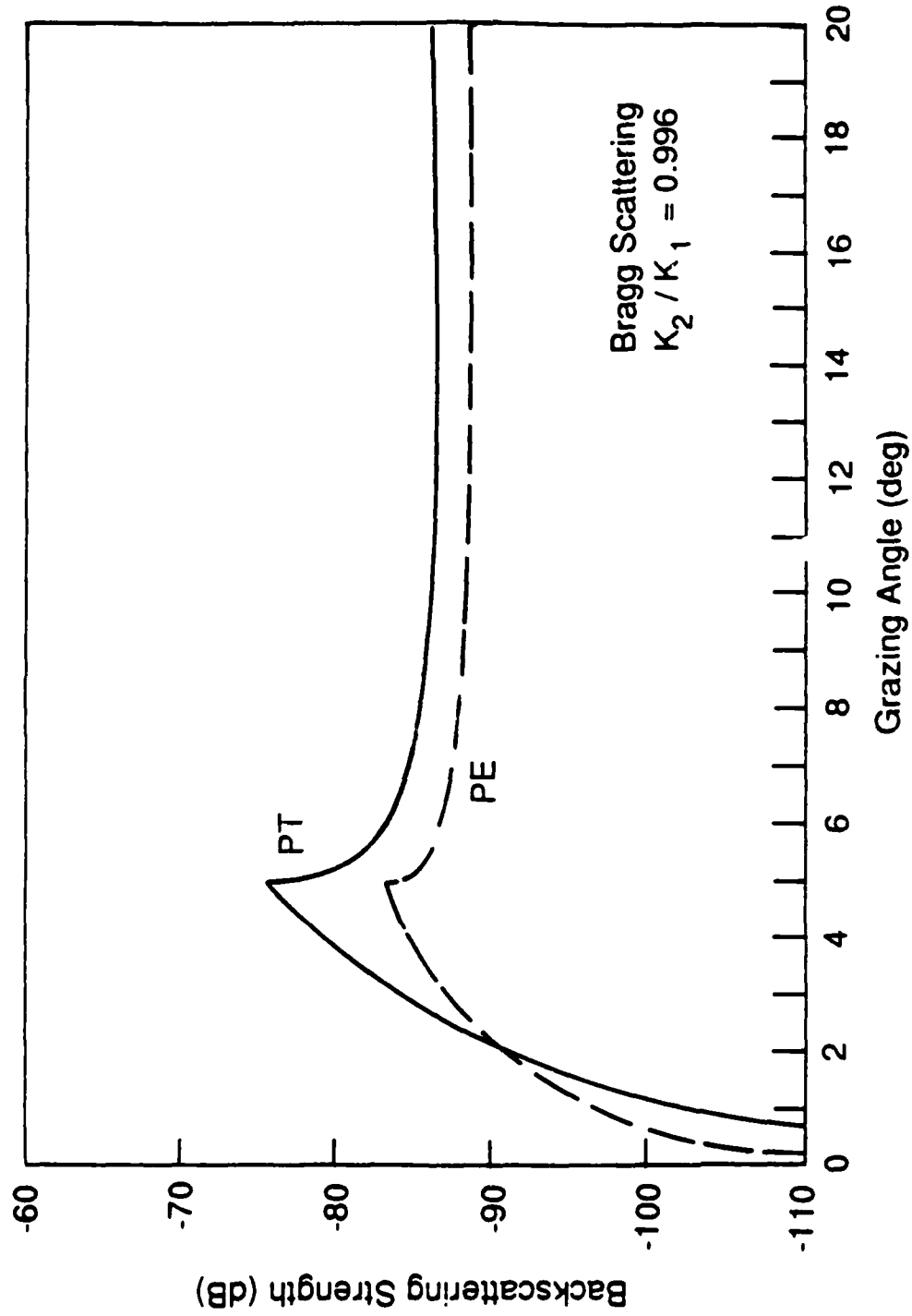


Figure 4. Comparison of PE and PT Bragg Backscatter for a Critical Angle of Five Degrees.

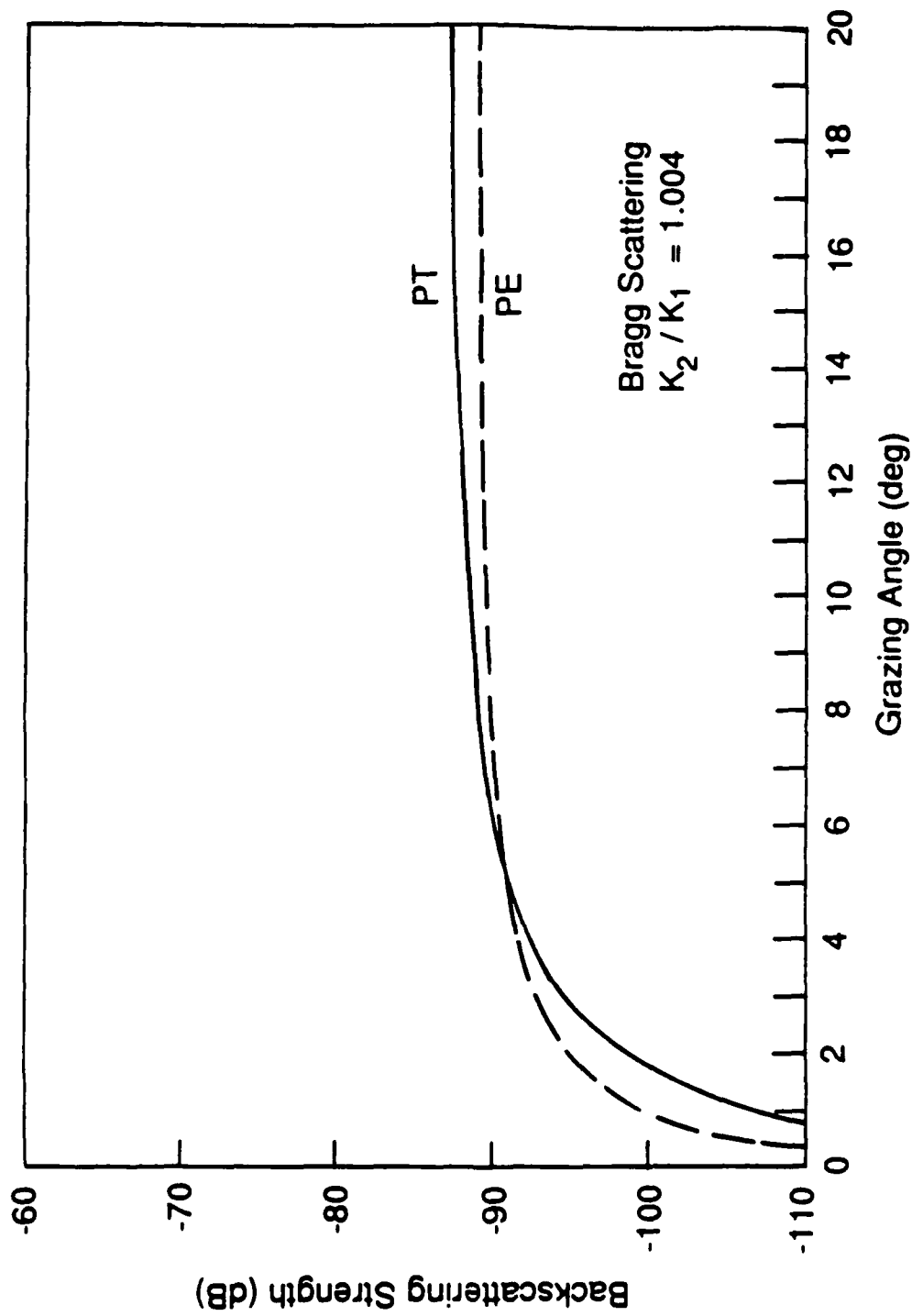


Figure 5. PE vs PT Bragg Backscatter for an Angle of Intrmission of Five Degrees.

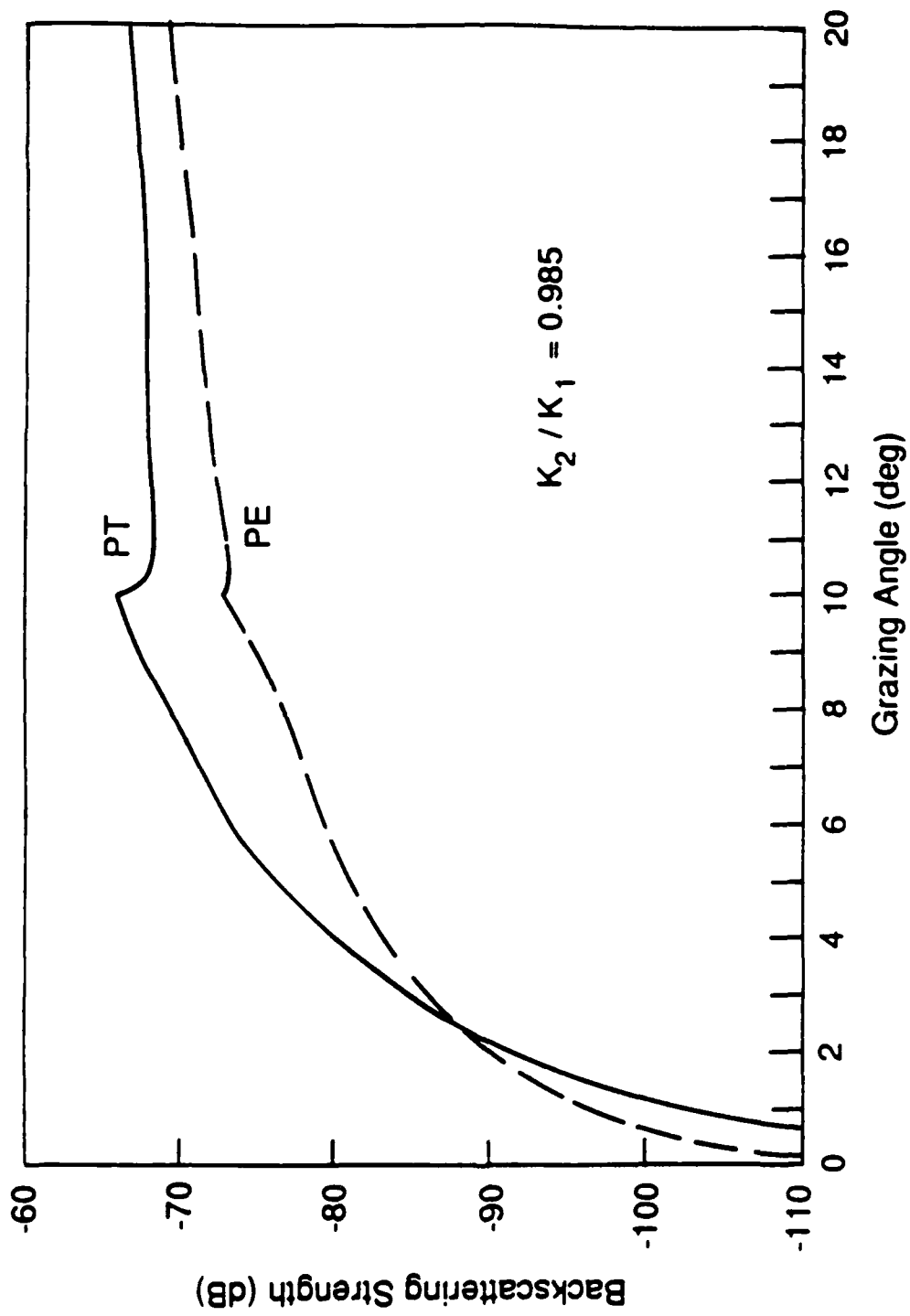


Figure 6. Higher Order (2,2) Contributions to Backscatter for a Critical Angle of Ten Degrees.

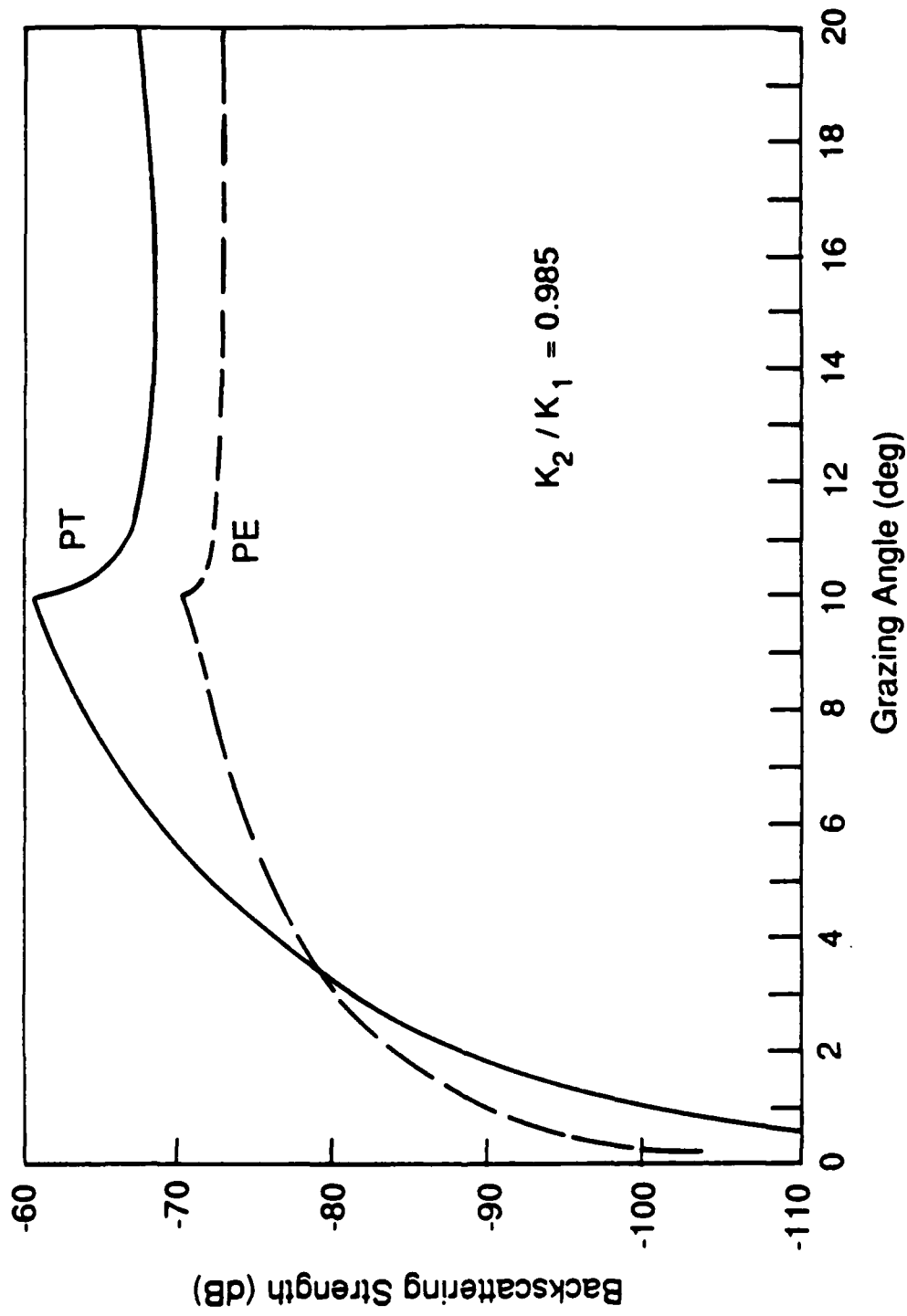


Figure 7. Fourth Order Backscattering Strength Predictions for a Critical Angle of Ten Degrees.

Distribution List for Unclassified ARL Penn State TM 91-104, entitled, "Backscattering from Rough Interfaces and the Parabolic Approximation," by S. T. McDaniel, dated 12 April 1991.

Scientific Officer Code 1125AO
Office of Naval Research
800 North Quincy Street
Arlington, VA 22217-5000

Attn: M. H. Orr - Code 1125AO
Copies No. 1-3

Applied Physics Laboratory
University of Washington
1013 N. E. 40th. Street
Seattle, WA 98105

Attn: Eric H. Thorsos
Copy No. 25

Administrative Grants Officer
Office of Naval Research
Administrative Contracting Officer
The Ohio State Univ. Research Ctr.
1314 Kinnear Road
Columbus, OH 43212-1194

Attn: Resident Representative N66005
Copy No. 4

Office of Naval Research
800 North Quincy Street
Arlington, VA 22217

Attn: Ralph Baer - Code 1125AO
Copy No. 26

Director
Naval Research Laboratory
Washington, DC 20375

Attn: Code 2627
Copies No. 5-10

The Pennsylvania State University
Mechanical Engineering Department
University Park, PA 16801

Attn: Alan Pierce
Copy No. 27

Defense Technical Information Center
Building 5, Cameron Station
Alexandria, VA 22314

Copies No. 11-22

Applied Research Laboratory
The Pennsylvania State University
Post Office Box 30
State College, PA 16804

Attn: ARL Library
Copy No. 28

Naval Underwater Systems Center
New London, CT 06320

Attn: Ding Lee - Code 3332
Copy No. 23

Naval Ocean and Atmospheric
Research Laboratory
Stennis Space Center, MS 39529-5004

Attn: Stanley Chin Bing - Code 221
Copy No. 24